Acta Med. Okayama, 2013
Vol. 67, No. 3, pp. 153–164

Acta Medica Okayama
http://escholarship.lib.okayama-u.ac.jp/amo/

Original Article

Improvement of the Efficacy of 5-aminolevulinic Acid-mediated Photodynamic Treatment in Human Oral Squamous Cell Carcinoma HSC-4

Masanao Yamamoto[a,d]*, Hirofumi Fujita[a], Naoki Katase[b], Keiji Inoue[c], Hitoshi Nagatsuka[b], Kozo Utsumi[a], Junzo Sasaki[a], and Hideyo Ohuchi[a]

Departments of [a]Cytology and Histology, [b]Oral Pathology, Okayama University Graduate School of Medicine, Dentistry and Pharmaceutical Sciences, Okayama 700–8558, Japan,
[c]Department of Urology, Kochi University Medical School, Nankoku, Kochi 783–8505, Japan,
[d]Department of Dysphagia Rehabilitation and Community Dental Care, Tokyo Dental College, Chiba 261–8502, Japan

Ever since protoporphyrin IX (PpIX) was discovered to accumulate preferentially in cancer cells after 5-aminolevulinic acid (ALA) treatment, photodynamic treatment or therapy (PDT) has been developed as an exciting new treatment option for cancer patients. However, the level of PpIX accumulation in oral cancer is fairly low and insufficient for PDT. Ferrochelatase (FECH) and ATP-binding cassette transporter G2 (ABCG2) are known to regulate PpIX accumulation. In addition, serum enhances PpIX export by ABCG2. We investigated here whether and how inhibitors of FECH and ABCG2 and their combination could improve PpIX accumulation and PDT efficacy in an oral cancer cell line in serum-containing medium. ABCG2 inhibitor and the combination of ABCG2 and FECH inhibitors increased PpIX in the presence of fetal bovine serum (FBS) in an oral cancer cell line. Analysis of ABCG2 gene silencing also revealed the involvement of ABCG2 in the regulation of PpIX accumulation. Inhibitors of FECH and ABCG2, and their combination increased the efficiency of ALA-PDT even in the presence of FBS. ALA-PDT-induced cell death was accompanied by apoptotic events and lipid peroxidation. These results suggest that accumulation of PpIX is determined by the activities of ABCG2 and FECH and that treatment with a combination of their inhibitors improves the efficacy of PDT for oral cancer, especially in the presence of serum.

Key words: 5-aminolevulinic acid, protoporphyrin IX, oncology, photodynamic therapy, apoptosis

5-aminolevulinic acid (ALA)-derived protoporphyrin IX (PpIX) has been shown to accumulate preferentially in cancer cells and proliferating normal cells by a regulatory mechanism specific to these cells [1]. When the accumulated PpIX, which is a fluorescent photosensitizer, is activated by visible light, cytotoxic reactive oxygen species (ROS) are generated and induce cell death in cancer cells. Thus, its application for photodynamic diagnosis (PDD) and treatment or therapy (PDT) for cancer patients has been developed in various fields [2–4]. However, the amount of ALA-induced PpIX accumulation in oral squamous cell carcinoma (OSCC) cells was found to be low, and PDT has been shown to be less than satisfactory *in vivo* [5, 6]. PpIX accumulation in ALA-treated cells is regulated by various factors such as

Received August 28, 2012; accepted December 6, 2012.
*Corresponding author. Phone:+81–86–235–7083; Fax:+81–86–235–7079
E-mail:gmd421001@s.okayama-u.ac.jp (M. Yamamoto)

1) uptake of added ALA [7], 2) metabolism of heme synthesis, such as 5-ALA-hydratase [8], porphobilinogen deaminase (PBGD) [8, 9], ferrochelatase (FECH) [7, 10], and heme oxygenase (HO) [11, 12], and 3) transport of heme intermediates, such as ABCB6 and ATP-binding cassette transporter G2 (ABCG2) [13–15]. It has been reported that ABC transporters efflux photosensitizers, and that ABCG2 inhibitors, such as fumitremorgin C (FTC), increase the intracellular PpIX [16].

As pre-malignant and malignant lesions of the oral cavity also preferentially accumulate ALA-induced PpIX and are accessible by laser light, they are suitable sites for PDD and PDT [5]. It has been noted that many of the *in vitro* PDT investigations have been carried out in serum-free culture medium, even though the microcirculation around tumor cells *in vivo* contains plasma that leaks out from blood vessels [17]. We previously reported that serum suppressed intracellular ALA-induced PpIX accumulation in human urothelial carcinoma cell line T24 due to the action of ABCG2, which exports the PpIX into extracellular space [18]. These findings suggest that the low level of PpIX accumulation in OSCC may be due to the suppression of PpIX accumulation by plasma. However, the effect of serum on the PpIX accumulation in OSCC cells has not been fully investigated. Thus, it is desirable to carry out experiments in serum-containing medium to analyze the mechanism of PDT.

As for the cell-death mechanism of ALA-PDT, 2 pathways have been proposed. One is the mitochondrial pathway and the other is an endoplasmic reticulum stress-induced pathway [19]. It was observed that ALA-PDT-treated K562 cells exhibited early apoptotic events, such as dissipation of mitochondrial membrane potential and mitochondrial cytochrome c release, but not late apoptotic events, such as caspase-3 activation or DNA fragmentation [20]. The cells eventually died by necrosis through plasma membrane damage. Moreover, PpIX was found to sensitize the cells to apoptosis when it existed mainly in the mitochondria and to necrosis when it diffused into other cellular sites, including the plasma membrane [21]. These findings point to the complexity of ALA-PDT in cancer cells.

In the present work, we describe the improvement of ALA-induced PpIX accumulation in HSC-4, an OSCC cell line, using various inhibitors of FECH and ABCG2, and improved the efficacy of ALA-enhanced PDT in the presence of serum in OSCC.

Materials and Methods

Chemicals. ALA and FTC were purchased from COSMO OIL (Tokyo, Japan). Deferoxamine (DFX), Annexin V-FITC, FBS, and propidium iodide (PI) were obtained from Sigma (St. Louis, MO, USA). FTC, (Z)-1-[N-(2-Aminoethyl)-N-(2-ammonioethyl)-mino]diazen-1-ium-1, 2-diolate (NOC18), and swallow-tailed perylene derivative of lipid hydroperoxide (Spy-LHP) were obtained from Alexis Biochem and Dojindo (Kumamoto, Japan). 10-Nonyl acridine orange (NAO) and tetramethylrhodamine-ethyl-ester (TMRE) were obtained from Molecular Probes (Eugene, OR, USA). The monoclonal antibody to ABCG2 was obtained from Cell Signaling Technology (Danver, MA, USA). The FECH antibody was donated by Dr. Taketani (Kyoto Institute of Technology, Japan). All other chemicals were of analytical grade and obtained from Nacalai Tesque (Tokyo, Japan). NAO and TMRE were dissolved in DMSO and stored in aliquots at 4℃ until use.

Cell culture and ALA treatment. HSC-2 and HSC-4 were provided by RIKEN Bio Resource Center. They were maintained in DMEM (Wako, Osaka, Japan) supplemented with 10% FBS, 100U/ml penicillin, and 100μg/ml streptomycin. Cells were cultured in a humidified atmosphere with 5% CO_2 at 37℃ as described previously [22]. The HSC-4 cells (1.5×10^5 cells) were cultured in media containing various concentrations of ALA in the presence or absence of 10% FBS.

Fluorescence microscopy. HSC-4 cells were seeded in 3.5-cm dishes and cultured in media containing various concentrations of ALA (0–2mM) with or without 300μM DFX, 300μM Noc-18, and 10μM FTC in the presence or absence of 10% FBS for 3h. After treatment with the indicated concentration of ALA for 3h, HSC-4 cells were stained with 10nM NAO for 10min at 37℃ and then observed by fluorescence microscopy (Zeiss, Axiovert 200) with a 100-W halogen lamp. Fluorescence images were taken using a highly light-sensitive thermo-electrically cooled charge-coupled device camera (ORCAII-ER, Hamamatsu, Japan). NAO for detection of mitochondria, a G365-nm excitation filter, a FT580-nm beam

splitter, and an up-to-LP590-nm emission filter for PpIX were also used [22, 23].

Exposing light and PDT analysis. In the presence of FBS, HSC-4 cells were incubated with 1.0 mM ALA at 37℃ for 3 h in the presence or absence of 10 μM FTC and 300 μM Noc18, then exposed to light for 20 min. Then, we changed the medium and cultured at 37℃ for 6 h in the presence of FBS. Next, the cells were stained with Annexin V/PI or TMRE and analyzed using a flow cytometer. As a light source, an Na-Li lamp (TheraBeam VR630, USHIO, Tokyo, Japan) was used. The wavelength of light was 600–700 nm. The light intensity was 9.6 J/cm^2 [22–24]. ALA-PDT-treated cells were stained using a TACS^{TM} Annexin V/PI Apoptosis Detection kit (Trevigen) and 100 μM TMRE, according to the manufacturer's instructions. Then, the cells were analyzed by flow cytometry.

The 100 μM z-VAD-fmk was applied at the same time as ALA application and FBS(+) medium change, then reapplied with FBS(+) medium. After 6 h, the proportion of cell death, apoptotic and necrotic cells was measured by flow cytometry.

Lipid peroxidation by ALA-PDT of cells was analyzed as previously described using a new fluorescent probe, Spy-LHP [23, 25, 26], which reacted rapidly and quantitatively with lipid hydroperoxides to form the corresponding oxide, Spy-LHPOx, which emits extremely strong fluorescence in the visible range (em = 535–574 nm). In the presence of FBS, HSC-4 cells were incubated with 1.0 mM ALA at 37℃ for 3 h in the presence or absence of 10 μM FTC and 300 μM Noc18, exposed for 20 min to light, and cultured at 37℃ for 10 min in the presence of FBS medium. Cells were incubated with 1 μM Spy-LHP for 10 min before ALA-PDT. Then, the cells were analyzed using a flow cytometer (FL1).

Flow cytometric analysis. Upon incubation with ALA, the cells grown on dishes were removed by treatment with trypsin. ALA-treated cells were filtered through a 50-μm nylon mesh (SEFER, Heiden, Switzerland). Then, the fluorescence intensity of the cells was measured using a Fluorescence-Activated Cell Sorter (BD, CA, USA). A total of 10,000 cells were analyzed for each sample (ex/em = 488/650 nm) [10, 22, 23]. PpIX was measured by flow cytometry using FACScan FL3-H.

Western blotting analysis. Cell specimens were subjected to SDS-polyacrylamide gel electrophoresis and proteins in the gel were transferred electrophoretically onto an Immobilon membrane (Millipore, Waltham, MA, USA). This membrane was probed with primary antibodies (1 : 1,000 mouse anti-human actin antibody, 3 : 1,000 rabbit anti-human ABCG2 antibody, 1 : 100 rabbit anti-bovine FECH antibody) and secondary antibodies using the SNAP i.d. system (Millipore), according to the manufacturer's instructions. Immunoreactive bands were visualized using an ECL system (Amersham Biotech, Uppsala, Sweden) [23].

RT-PCR analysis. To determine the expression of ferrochelatase and ABCG2 transcriptions, RT-PCR was performed as follows. Total RNA was isolated from cells using TRIzol (Invitrogen) following the manufacturer's instructions. Oligo dT-primed cDNA was prepared from 1 ug of total RNA using Superscript II (Invitrogen). One-twentieth of each obtained cDNA specimen was used for PCR. Primers were designed on the basis of sequences of human ferrochelatase [27], human ABCG2 [28], and human acidic ribosomal phosphoprotein 36B4 [29, 30]. 36B4 is a housekeeping gene that is expressed constantly in tissue. Amplification of ferrochelatase, ABCG2, and the positive control 36B4 was carried out using forward primer 5'-CGCAGAAGAGGA AGCCGAAAAC-3' and reverse primer 5'-GGTCGC CTCTGTTGACCACAGA-3' for ferrochelatase, forward primer 5'-GATCTCTCACCCTGG GGCTTGTGGA-3' and reverse primer 5'-TGTGCA ACAGTGTGATGCAAGGGA-3' for ABCG2, and forward primer 5'-TGCCAGTGTCTGTCTGCAGA -3' and reverse primer 5'-ACAAAGGCAGATGGA TCAGC-3' for 36B4. The PCR reaction was carried out with an initial period at 95℃ for 4 min, then 35 cycles at 95℃ for 1 min, 60℃ for 1 min, and 72℃ for 1 min. The PCR products were separated by 1.2% (w/v) agarose gel electrophoresis and detected with ethidium bromide under UV light.

ABCG2 siRNA transfection. Three different Stealth ABCG2 siRNA duplexes (Invitrogen) were used in combination with transient inhibition of ABCG2 gene expression in HSC-4 cells as described previously [31]. HSC-4 cells were incubated with lipofectamine RNAi MAX transfection reagent according to the reverse transfection protocol provided by the manufacturer. Stealth ABCG2 siRNA

was used as a pool in equal proportions at a final concentration of 50 nM.

Statistical analysis. Statistical analysis was carried out using Student's t test (SPSS 11.0 for Windows). Results are expressed as means ± SDs, and p values < 0.05 were considered to indicate significant differences.

Results

Accumulation of PpIX in ALA-treated OSCC. To confirm the effect of serum on intracellular PpIX accumulation in OSCC cell lines, cells from HSC-4, a human tongue carcinoma cell line, and HSC-2, a human oral squamous carcinoma cell line, were treated with ALA in the presence and absence of FBS (Fig. 1). As shown in Figs. 1A and B, the accumulation of intracellular PpIX in these cell lines

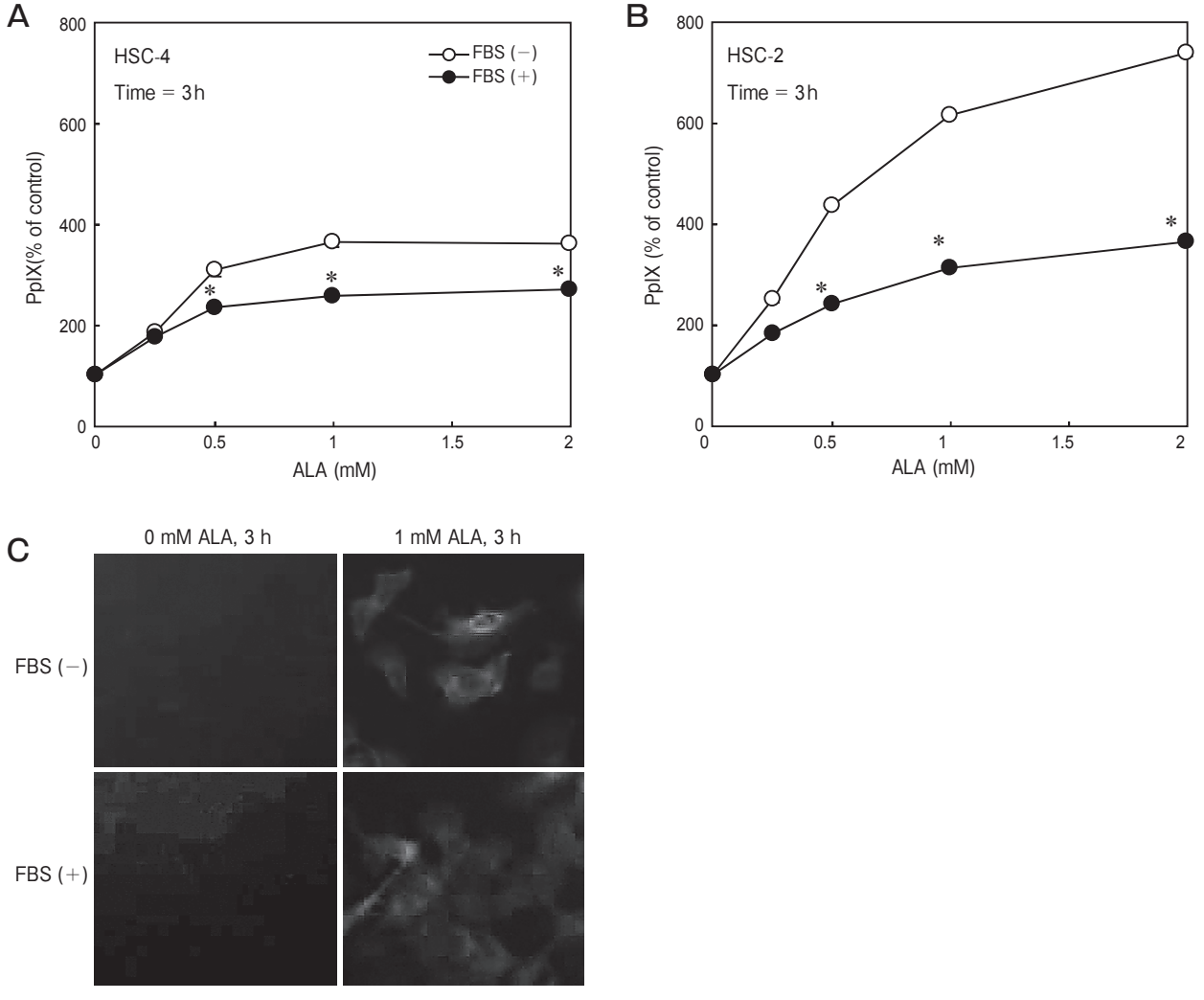

Fig. 1 ALA-mediated PpIX accumulation in OSCC. (**A**, **B**) Accumulation of ALA-induced PpIX in HSC-4 and HSC-2 cells after incubation with the indicated concentrations of ALA in the presence or absence of FBS for 3h. HSC-4 (A) and HSC-2 (B) cells were exposed to 0–2.0 mM ALA for 3h. PpIX accumulation was analyzed by flow cytometry. Filled and open circles show the PpIX values in the presence and absence of serum, respectively. Values are the means ± SDs derived from three independent experiments. Asterisks indicate significant differences from the corresponding FBS(−) samples. (**C**) Accumulated PpIX was observed by fluorescence microscopy after ALA treatment in the absence or presence of FBS. Merged pictures (mitochondria and PpIX) are shown.

was increased in an ALA dose-dependent manner, and the accumulations in the presence of FBS were significantly reduced compared with those in the absence of FBS (at 1.0 mM, 30% decrease in HSC-4, 50% decrease in HSC-2). The PpIX accumulation in HSC-4 was lower than that in HSC-2. Fig. 1C shows the accumulated PpIX in HSC-4 cells, observed by fluorescence microscopy. Since the aim of this study was to improve PDD and PDT in oral cancer cells having low capacity for PpIX accumulation in the presence of serum, the subsequent experiments were performed with HSC-4.

Enhancement of PpIX accumulation by the inhibitors FECH and ABCG2 and their combination. Heme biosynthesis by FECH, which is a NO-sensitive enzyme, requires iron and PpIX as substrates; then the iron chelator DFX and NO donor NOC18 can increase the intracellular ALA-induced PpIX accumulation [10, 32]. In addition, since ABCG2 exports PpIX, its specific inhibitor FTC effectively increases the intracellular PpIX [14]. Thus, we investigated whether FECH and ABCG2 inhibitors and their combination could improve the ALA-induced PpIX accumulation in HSC-4. First, we confirmed the gene and protein expression of FECH and ABCG2 in HSC-4 (Fig. 2A and B). Both mRNA and protein expressions of FECH and ABCG2 were detected in HSC-4 cells.

In the absence of serum, both DFX and Noc18, but not FTC, significantly increased the PpIX accumulation, by 5.0- and 5.2-fold, respectively (Fig. 2C). In contrast, in the presence of serum, FTC but neither DFX nor Noc18, significantly increased the PpIX accumulation, by 2.9-fold (Fig. 2D). The combination of FTC and Noc18 strongly enhanced PpIX accumulation in HSC-4 in both the presence (4.4-fold) and absence (11.2-fold) of serum.

To confirm visually the increase of intracellular PpIX by FECH and ABCG2 inhibitors in HSC-4 cells, intracellular PpIX was assessed by fluorescence microscopy (Fig. 2E). We used NAO to detect the mitochondria. In the absence of FBS, Noc18 increased the accumulation of PpIX. DFX also induced a similar increase (data not shown). In contrast, in the presence of FBS, FTC increased the accumulation of PpIX, and related intracellular distributions were observed in the mitochondria and cytosol. Thus, it seems that PpIX export by ABCG2 in the presence of serum is a major determinant of PpIX accumulation in HSC-4.

Effect of ABCG2 gene silencing on intracellular PpIX accumulation in HSC-4. To determine whether ABCG2 plays a critical role in the efflux of PpIX in HSC-4 cells, we developed a washing method for the release of accumulated PpIX from cells after incubation with ALA (Fig. 3). Fig. 3A shows the experimental procedure. First, we used ABCG2 siRNA transfection. We observed the largest silencing effect on ABCG2 mRNA expression by the transfection of 50 nM siRNA (Fig. 3B). Protein levels of ABCG2 were also downregulated by RNAi (Fig. 3C). Then, we used this siRNA concentration for a washing method.

Fig. 3D shows the effect of FTC, Noc18, and both on the amount of accumulated PpIX after washing cells with FBS-containing ALA-free medium. The accumulated PpIX decreased after washing the cells. The level of accumulated PpIX was increased by FTC and FTC + Noc18 in the presence of FBS. After the RNAi treatment, 1) the accumulated PpIX in ALA-treated cells did not decrease after washing the cells. Moreover, 2) treatment with Noc18 substantially increased the cellular level of PpIX (Fig. 3E). In contrast, 3) the effects of FTC and FTC + Noc18 on the PpIX level were about the same as those in Fig. 3D. These results indicated that ABCG2-mediated PpIX efflux might be an important pathway for the regulation of the PpIX level in FBS-containing medium in HSC-4 cells.

Enhancement of the efficacy of PDT by the combination of ABCG2 and FECH inhibitors. We next developed an experimental procedure to confirm the ALA-PDT effect in HSC-4 cells treated with ABCG2 and FECH inhibitors in the presence of FBS (Fig. 4A). ALA-PDT-induced cell death with various inhibitors was analyzed by a forward-scatter/side-scatter (FSC/SSC) scattergram using flow cytometry. We counted fewer FSC events, which reflect cell membrane fragmentation, cell shrinkage, and the formation of apoptotic bodies (Fig. 4B). Cell death was induced significantly by ALA-PDT with FTC, and the highest level of cell death was observed in ALA-PDT with FTC + Noc18 or FTC + DFX. Phosphatidylserine (PS) externalization, a feature of early apoptotic cell death, and disruption of cell membrane integrity, a feature of necrotic or late

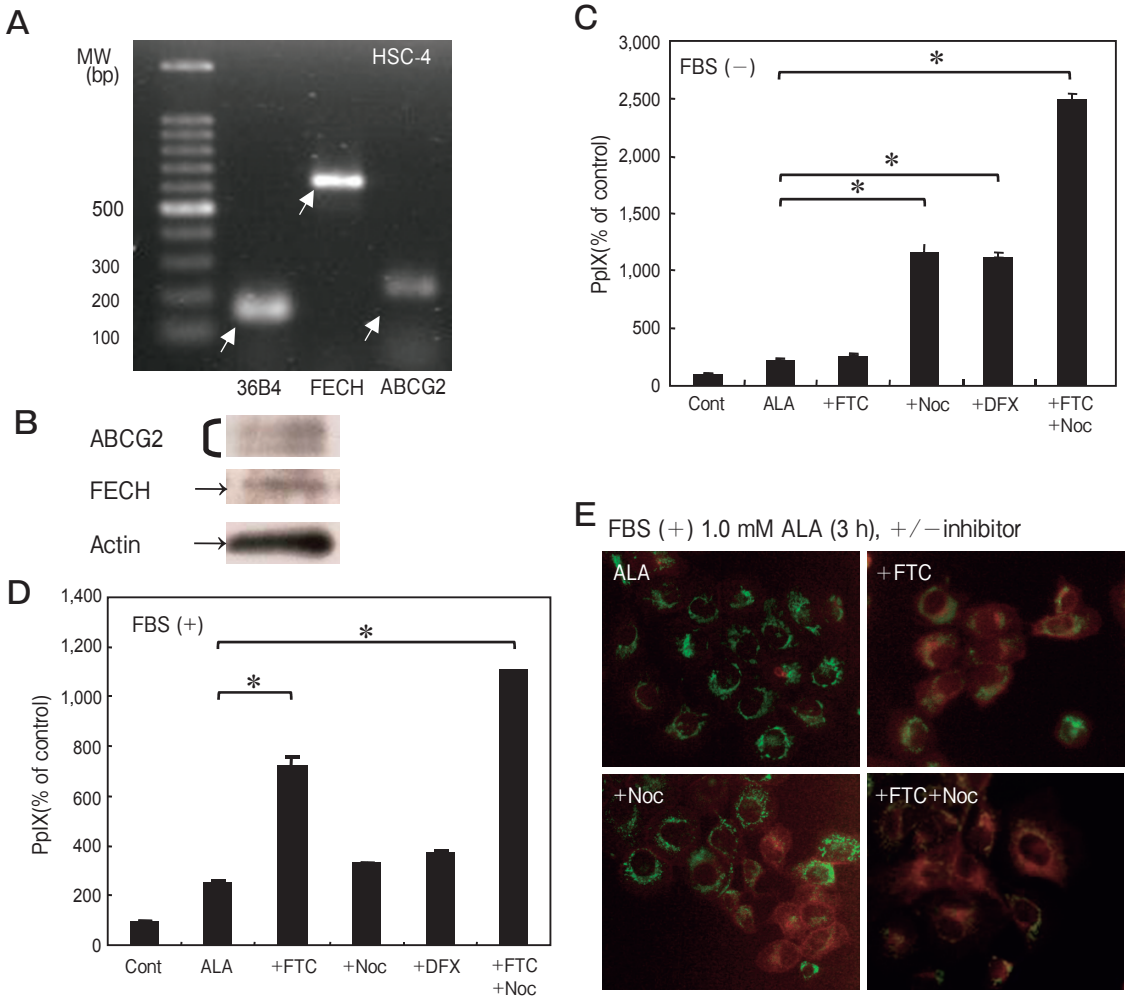

Fig. 2 Effect of ABCG2 and FECH inhibitors on PpIX accumulation in HSC-4 cells. (**A**) mRNA expressions of ABCG2 and FECH in HSC-4 were detected by RT-PCR. (**B**) Protein expressions of ABCG2 and FECH in HSC-4 were detected by western blotting. ABCG2: approx. 72kDa, FECH: approx. 42kDa, Actin: approx. 42kDa. (**C**, **D**) Effect of ABCG2 and FECH inhibitors and their combination on ALA-mediated PpIX accumulation in HSC-4 cells. HSC-4 cells were incubated with the indicated concentration of ALA with or without 300 μM DFX, 300 μM Noc-18, and 10 μM FTC for 3 h in the absence (C) or presence of FBS (D). PpIX accumulation was analyzed by flow cytometry. Values are the means ± SDs derived from three independent experiments. Asterisks indicate significant differences from the corresponding ALA samples. (**E**) Accumulated PpIX and mitochondria were observed by fluorescence microscopy after ALA and inhibitor treatment in the presence of FBS. Mitochondria were stained with NAO.

apoptotic cell death, were analyzed by Annexin-V/PI staining and flow cytometry. As shown in Fig. 4C and D, early apoptotic cell death by ALA-PDT was significantly promoted by FTC or DFX, and disruption of cell membrane integrity by ALA-PDT was also promoted by FTC. Furthermore, late apoptotic or necrotic cell death was strongly promoted by the combination of FECH and ABCG2 inhibitors in parallel with a decrease of FTC, as shown in Fig. 4B. In addition, we analyzed the changes in mitochondrial membrane potential in cells using TMRE staining, and observed depolarization of the membrane potential, which occurred in parallel with cell death (Fig. 4E). Figs. 4B-E show that ALA-PDT-induced cell death involves apoptosis.

Effect of z-VAD-fmk on ALA-PDT by the inhibitors ABCG2 and FECH and their combination. Next, we verified the potential of ALA-

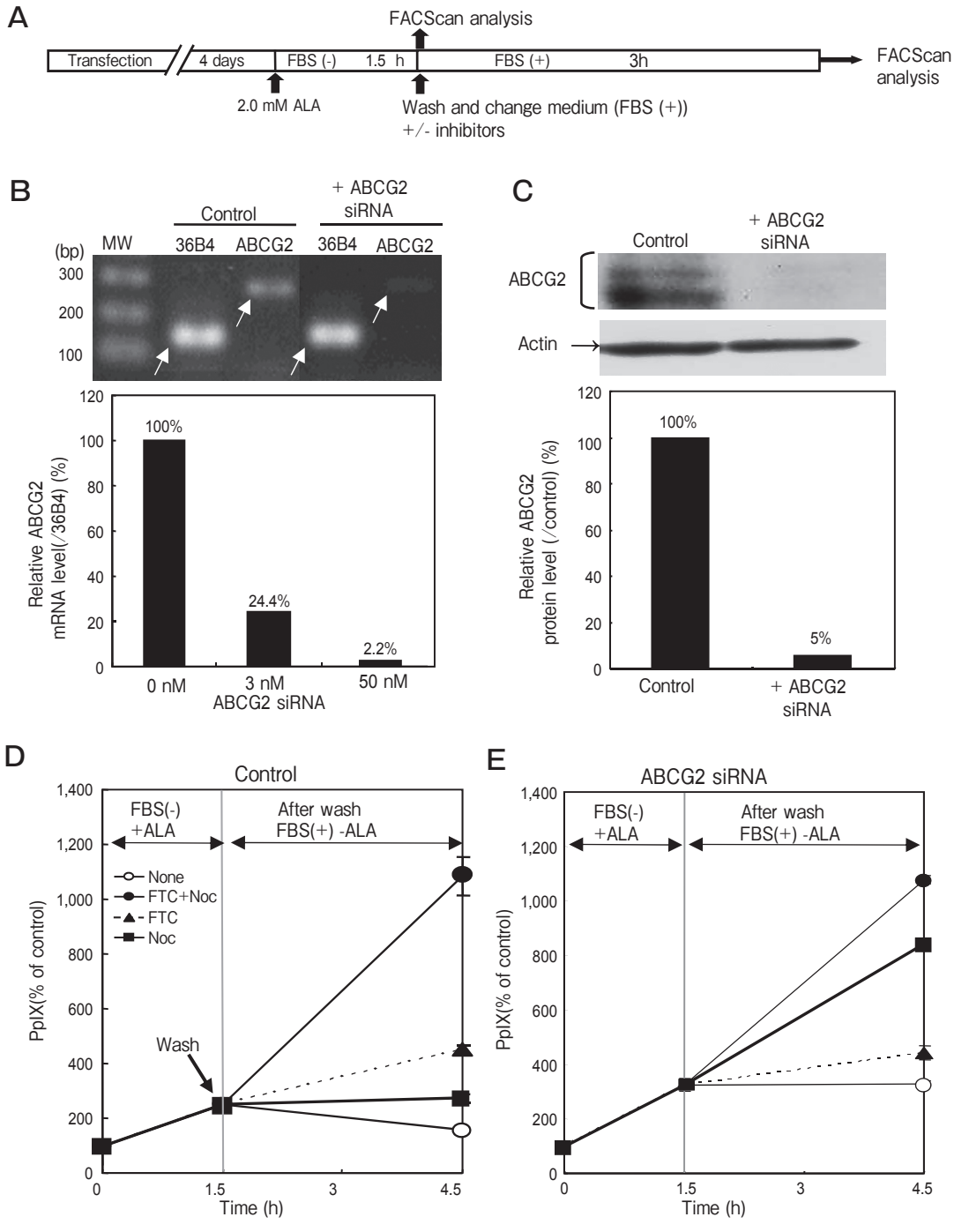

Fig. 3 Silencing of ABCG2 expression in HSC-4 cells and its effect on the sensitivity to FTC and/or Noc-18 in ALA-mediated PpIX accumulation. (**A**) Experimental schedule of ABCG2 gene silencing and ALA-mediated PpIX accumulation. (**B**) Expression of ABCG2 mRNA was detected by RT-PCR after 4 days of transfection with gene-specific siRNA. (**C**) Protein expressions of ABCG2 and FECH were detected by western blotting after 4 days of transfection. (**D**, **E**) HSC-4 cells were incubated with 2.0 mM ALA for 1.5 h in FBS-free culture medium, and the cells were washed with FBS-containing incubation medium in the presence or absence of 10 μM FTC or 300 μM Noc-18. The content of PpIX in the cells was measured using a flow cytometer. Cellular PpIX accumulation without (D) or with (E) siRNA transfection. Values are the means $\pm$ SD derived from 3 independent experiments.

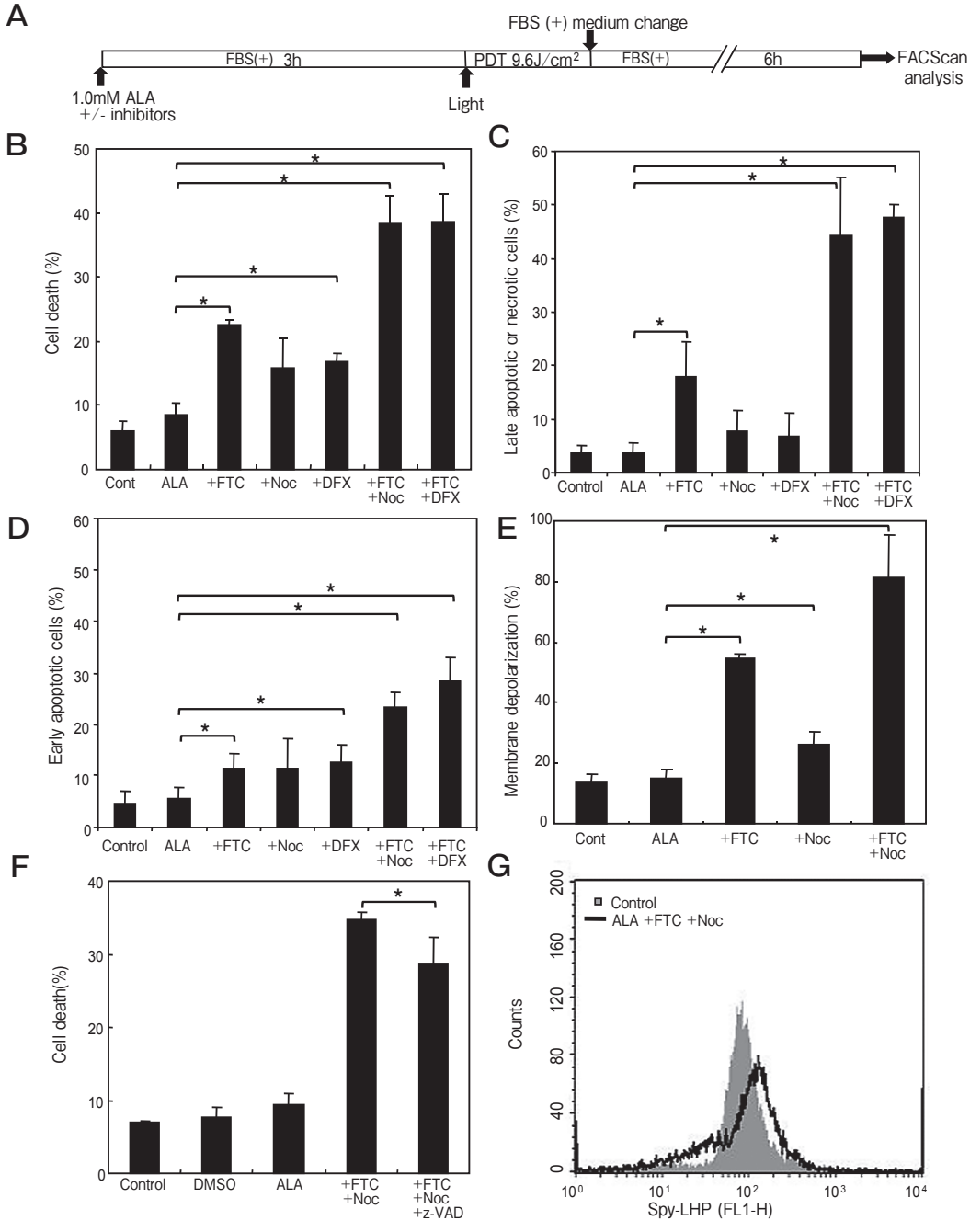

Fig. 4 Enhancement of ALA-PDT-induced cell death by ABCG2 and FECH inhibitors in combination in HSC-4. (**A**) Experimental schedule of PDT with the combination of ABCG2 and FECH inhibitors. (**B**) Presence of cell death in FSC/SSC plot after PDT. The FSC-decreased cells were defined as dead cells. Asterisks indicate significant differences from the corresponding ALA samples. (**C**, **D**) Cells were stained with Annexin V/PI after PDT and analyzed by flow cytometry. PS-externalized and PI-stained cells: late apoptotic or necrotic cells (C). Phosphatidylserine (PS)-externalized cells: early apoptotic cells (D). Values are the means ± SDs derived from 3 independent experiments. Asterisks indicate significant differences from the corresponding ALA samples. (**E**) Mitochondrial membrane potential was detected by TMRE staining after the ALA-PDT, and analyzed by flow cytometry (FL-2). Values are the means ± SDs derived from 3 independent experiments. Asterisks indicate significant differences from the corresponding ALA samples. (**F**) Effect of pan-caspase inhibitor z-VAD-fmk on the ALA-PDT-induced cell death. Experimental schedule is the same as in (B). The proportion of cell death was measured by flow cytometry. Values are the means ± SDs derived from 3 independent experiments. Asterisks indicate significant differences from the corresponding+FTC+Noc-18 samples. (**G**) Lipid peroxidation. The cells were subsequently analyzed using a flow cytometer.

PDT-induced cell death to involve the apoptotic pathways. To investigate whether caspases play a role in the cell death that follows ALA-induced PDT, the effect of PDT on cell death was evaluated in the absence and presence of the pan-caspase inhibitor z-VAD-fmk (Fig. 4F). The proportion of cell death was significantly decreased in the presence of z-VAD-fmk (20% decrease), suggesting the involvement of a caspase-dependent apoptotic pathway in this cell death mechanism.

Induction of lipid peroxidation in ALA-PDT by the combination of ABCG2 and FECH inhibitors. It was reported that PDT produces a singlet oxygen and induces lipid peroxidation *in vitro* and that photodynamic peroxidation of cellular lipids is a consequence of PDT associated with cytolethality. To examine the effect of PDT on lipid peroxidation, we used Spy-LHP. The fluorescence intensity of Spy-LHP was increased a short time after PDT, suggesting the involvement of lipid peroxidation at an early stage of this cell death mechanism (Fig. 4G).

Discussion

The OSCC cell line HSC-4 showed a low level of ALA-induced PpIX accumulation, and the efficacy of ALA-PDT in the cells was insufficient. The combination of inhibitors of heme synthesis and ABCG2 improved the accumulation and efficacy of ALA-PDT in HSC-4, especially by the inhibition of PpIX release through ABCG2 in the presence of FBS (Fig. 5). Export of PpIX by ABCG2 might be a key factor in determining the efficacy of ALA-PDT in an *in vivo* environment of oral cancer. This is the first report on the efficacy of ABCG2, FECH inhibitors, and their combination for ALA-PDT in FBS-containing medium in OSCC cell lines. No report about this treatment has been previously published.

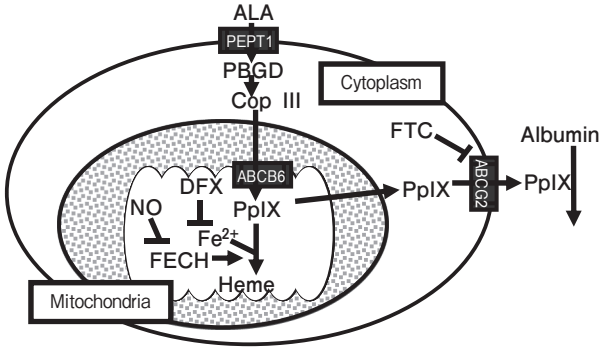

porphobilinogen deaminase (PBGD)
Coproporphyrinogen III (Cop III)
Peptide transporter 1 (PEPT1)

Fig. 5 Schematic representation of the mechanism of ALA-mediated PpIX accumulation improved by the combination of ABCG2 and FECH inhibitors in HSC-4.

Previously, the amount of ALA-induced PpIX in OSCC was found to be low, and PDT in oral cancer patients has been unsatisfactory [5, 6]. It has also been shown that several factors are involved in the regulation of ALA-induced PpIX accumulation and that the decrease of intracellular PpIX is regulated by the PpIX metabolic pathway and efflux pathways [4–10, 33, 34]. FECH is the terminal enzyme of the heme-biosynthetic pathway and is thought to be the rate-limiting step for heme synthesis. ABCG2 is a transporter in the cell membrane for heme intermediates and is thought to regulate the traffic of PpIX in the presence of serum. In this study, ABCG2 and FECH inhibitors and their combination improved the ALA-induced PpIX accumulation in OSCC. These findings suggested that the combination of ABCG2 and FECH inhibitors might improve the efficacy of ALA-PDT in oral cancer patients.

It has been reported that ABCG2 is localized at the plasma membrane and provides a mechanism to remove excess porphyries to maintain intracellular porphyry homeostasis and that ABCG2 acted to modulate porphyry concentrations under normal conditions [17]. Thus, ABCG2 can appropriately control the level of intracellular PpIX. The present study is the first to reveal the involvement of ABCG2 in ALA-mediated PpIX accumulation in medium containing FBS using knockdown of ABCG2 in HSC-4 (Fig. 3). These findings indicated that the increase of ALA-mediated PpIX accumulation in cancer cells by ABCG2 inhibitors is important, especially for clinical applications. In this context, several findings have previously been made on the effects of serum and ABC transporters on PpIX accumulation in ALA-treated cells: 1) Serum inhibited the PpIX accumulation in several cells [35–37]; 2) Serum increased the release of accumulated PpIX to extracellular space [38, 39]; 3) Serum induced a different localization of synthesized PpIX in ALA-treated cells [40]; 4) ABCG2-expressing cells accumulated a low level of ALA-mediated PpIX [41];

5) An ABCG2 inhibitor suppressed the export of PpIX from cells to the extracellular space and increased the PpIX accumulation [14]; 6) ABCG2 mediated the transport of photosensitizers [16]; 7) Both PpIX and heme bound to the ECL3 (ABCG2 large extracellular loop) region in transmembrane spans 5 and 6 of ABCG2, and human serum albumin could be one of the possible partners for its removal [42]; and 8) PpIX bound to BSA [33]. On the basis of these findings, it was concluded that ALA-PDT was strongly enhanced by the FECH inhibitor in combination with that of ABCG2 (Fig. 4). This could be a new method to improve photodynamic therapy for OSCC. Recently, it was reported that ABCG2 was distributed not only in the cell membrane but also in the inner membrane of mitochondria [34] and that the ABCG2 protein is sensitive to FTC. Thus, further study is required to clarify the role of ABCG2 in the molecular mechanism of PpIX accumulation in various cells including HSC-4 cells.

It is preferable to induce the apoptotic rather than necrotic cell death of target cancer cells by PDT because apoptotic cell death does not affect the adjacent normal cells. Previously, it was reported that the subcellular localization of PpIX might affect the type of cell death, *i.e.*, apoptosis or necrosis [23]. Light exposure of cells containing PpIX, which was distributed in the mitochondria or the cytosol, induced apoptosis and necrosis, respectively, in an epithelial breast tumor line [21]. It was also reported that ALA-PDT induced apoptotic cell death in human oral cancer Ca9-22 cells [43]. In this experiment, the distributions of accumulated PpIX by treatment with ABCG2 inhibitor and a combination of ABCG2 and FECH inhibitors were observed in the cytosol and mitochondria of HSC-4 (Fig. 2), and both apoptosis and necrosis could be induced after ALA-PDT with the combination of these inhibitors (Fig. 4). In addition, a pan-caspase inhibitor suppressed only 20% of the cell death. In this context, it was reported that both caspase-dependent and -independent apoptotic cell death was induced by ALA-PDT in human lymphoma cells [44]. These findings suggested that the major part of PDT-induced cell death promoted by the combination of ABCG2 and FECH inhibitors was caspase-independent apoptotic cell death and/or necrotic cell death. Necrotic cell death could lead to inflammation in the surrounding tissue. Thus, improvement of the rate of necrotic cell death among the total cell death is our next subject for study.

Apoptosis also occurred at least partly in HSC-4 cells after ALA-PDT, and the apoptotic process may be induced by the loss of mitochondrial function. In this context, there was evidence of mitochondrial swelling accompanied by loss of mitochondrial membrane integrity and autophagic vacuolization of the cytoplasm [45]. Reactive oxygen species scavengers delay the progression of mitochondrial depolarization and apoptotic cell death [46]. In this study, we observed membrane potential depolarization and increased lipid peroxidation after ALA-PDT with the combination of ABCG2 and FECH inhibitors. However, a preliminary experiment showed no autophagic change. In addition, ALA-PDT-induced apoptosis with the combination of ABCG2 and FECH inhibitors was suppressed by the pan-caspase inhibitor zVAD-FMK. These findings showed that cell death induced by ALA-PDT with the combination of ABCG2 and FECH inhibitors in HSC-4 was accompanied by mitochondrial depolarization and lipid peroxidation, which is a zVAD-FMK-inhibitable mechanism. Taking these findings together, we propose the following causal sequence of apoptosis induced by ALA-PDT with the combination of inhibitors in HSC-4: i) intracellular generation of ROS such as singlet oxygen by ALA-PDT is the initial event; ii) lipid peroxidation by the ROS induces mitochondrial membrane disruption accompanied by mitochondrial depolarization; iii) cytochrome c is probably released from mitochondria, activating the caspase cascade; and (iv) this cascade induces chromatin condensation and PS externalization. On the other hand, singlet oxygen and lipid peroxide induction by ALA-PDT might also induce the disruption of the plasma membrane, which in turn induces necrotic cell death.

A group of heme proteins, the cyclooxygenases (COXs), are key enzymes required for the conversion of arachidonic acid to prostaglandins. In addition, Karthein *et al.* reported the involvement of ferryl-PpIX in the catalytic mechanism of COX [47]. It was reported that COX-2 mRNA was detectable in the HSC2, but not in HSC-4 [48]. In this context, our results showed that the PpIX accumulation in HSC-2 was higher than in HSC-4. These findings suggest that the expression level of a heme protein, such as COX-2, is involved in the level of intracellular PpIX accu-

mulation.

The investigations reported in this paper have revealed a novel method to increase PpIX accumulation and improve the efficacy of ALA-PDT in HSC-4. These findings should promote the development of new anticancer therapeutic modalities.

Acknowledgments. We are very grateful to Dr. Taketani for donating the anti-FECH antibody used in our experiments. This work was supported by JSPS KAKENHI [grant number 20791042]. None of the authors has any conflicts of interest associated with this study.

References

1. Collaud S, Juzeniene J, Morn J and Lange N: On the selectivity of 5-aminolevulinic acid-induced protoporphyrin IX formation. Curr Med Chem Anticancer Agents (2004) 4: 301–316.
2. Peng Q, Warloe T, Berg K, Moan J, Kongshaug M, Giercksky KE and Nesland JM: 5-Aminolevulinic acid-based photodynamic therapy. Clinical research and future challenges. Cancer (1997) 79: 2282–2308.
3. Hinnen P, DE Rooij FW, VAN Velthuysen ML, Edixhoven A, van Hillegersberg R, Tilanus HW, Wilson JH and Siersema PD: Biochemical basis of 5-aminolaevulinic acid-induced protoporphyrin IX accumulation: a study in patients with (pre) malignant lesions of the oesophagus. Br J Cancer (1998) 78: 679–682.
4. Bartosová J and Hrkal Z: Accumulation of protoporphyrin-IX (PpIX) in leukemic cell lines following induction by 5-aminolevulinic acid (ALA). Comp Biochem Physiol C Toxicol Pharmacol (2000) 126: 245–252.
5. Konopka K and Goslinski T: Photodynamic therapy in dentistry. J Dent Res (2007) 86: 694–707.
6. Uekusa M, Omura K, Nakajima Y, Hasegawa S, Harada H, Morita KI and Tsuda H: Uptake and kinetics of 5-aminolevulinic acid in oral squamous cell carcinoma. Int J Oral Maxillofac Surg (2010) 39: 802–805.
7. Krieg RC, Fickweiler S, Wolfbeis OS and Knuechel R: Cell-type specific protoporphyrin IX metabolism in human bladder cancer in vitro. Photochem Photobiol (2000) 72: 226–233.
8. Gibson SL, Havens JJ, Metz L and Hilf R: Is delta-aminolevulinic acid dehydratase rate limiting in heme biosynthesis following exposure of cells to delta-aminolevulinic acid? Photochem Photobiol (2001) 73: 312–317.
9. Ickowicz Schwartz D, Gozlan Y, Greenbaum L, Greenbaum L, Babushkina T, Katcoff DJ and Malik Z: Differentiation-dependent photodynamic therapy regulated by porphobilinogen deaminase in B16 melanoma. Br J Cancer (2004) 90: 1833–1841.
10. Yamamoto F, Ohgari Y, Yamaki N, Kitajima S, Shimokawa O, Matsui H and Taketani S: The role of nitric oxide in delta-aminolevulinic acid (ALA)-induced photosensitivity of cancerous cells. Biochem Biophys Res Commun (2007) 353: 541–546.
11. Okimura Y, Fujita H, Ogino T, Inoue K, Shuin T, Yano H, Yasuda T, Inoue M, Utsumi K and Sasaki J: Regulation of 5-aminolevulinic acid-dependent protoporphyrin IX accumulations in human histiocytic lymphoma U937 cells. Physiol Chem Phys Med NMR (2007) 39: 69–82.
12. Frank J, Lornejad-Schäfer MR, Schöffl H, Flaccus A, Lambert C and Biesalski HK: Inhibition of heme oxygenase-1 increases responsiveness of melanoma cells to ALA-based photodynamic therapy. Int J Oncol (2007) 31: 1539–1545.
13. Krishnamurthy P, Xie T and Schuetz JD: The role of transporters in cellular heme and porphyrin homeostasis. Pharmacol Ther (2007) 114: 345–358.
14. Susanto J, Lin YH, Chen YN, Shen CR, Yan YT, Tsai ST, Chen CH and Shen CN: Porphyrin homeostasis maintained by ABCG2 regulates self-renewal of embryonic stem cells. (2008) PLoS One 3: e4023.
15. Zutz A, Gompf S, Schägger H and Tampé R: Mitochondrial ABC proteins in health and disease. Biochim Biophys Acta (2009) 1787: 681–690.
16. Robey RW, Steadman K, Polgar O and Bates SE: ABCG2-mediated transport of photosensitizers: potential impact on photodynamic therapy. Cancer Biol Ther (2005) 4: 187–194.
17. White MJ, Miller FN, Heuser LS and Pietsch CG: Human malignant ascites and histamine-induced protein leakage from the normal microcirculation. Microvasc Res (1988) 35: 63–72.
18. Ogino T, Kobuchi H, Munetomo K, Fujita H, Yamamoto M, Utsumi T, Inoue K, Shuin T, Sasaki J, Inoue M and Utsumi K: Serum-dependent export of protoporphyrin IX by ATP-binding cassette transporter G2 in T24 cells. Mol Cell Biochem (2011) 358: 297–307.
19. Grebenová D, Kuzelová K, Smetana K, Pluskalová M, Cajthamlová H, Marinov I, Fuchs O, Soucek J, Jarolím P and Hrkal Z: Mitochondrial and endoplasmic reticulum stress-induced apoptotic pathways are activated by 5-aminolevulinic acid-based photodynamic therapy in HL60 leukemia cells. J Photochem Photobiol B (2003) 69: 71–85.
20. Kuzelová K, Grebenová D, Pluskalová M, Marinov I and Hrkal Z: Early apoptotic features of K562 cell death induced by 5-aminolaevulinic acid-based photodynamic therapy. J Photochem Photobiol B (2004) 73: 67–78.
21. Kriska T, Korytowski W and Girotti AW: Role of mitochondrial cardiolipin peroxidation in apoptotic photokilling of 5-aminolevulinate-treated tumor cells. Arch Biochem Biophys (2005) 433: 435–446.
22. Inoue K, Karashima T, Kamada M, Shuin T, Kurabayashi A, Furihata M, Fujita H, Utsumi K and Sasaki J: Regulation of 5-aminolevulinic acid-mediated protoporphyrin IX accumulation in human urothelial carcinomas. Pathobiology (2009) 76: 303–314.
23. Amo T, Kawanishi N, Uchida M, Fujita H, Oyanagi E, Utsumi T, Ogino T, Inoue K, Shuin T, Utsumi K and Sasaki J: Mechanism of cell death by 5-aminolevulinic acid-based photodynamic action and its enhancement by ferrochelatase inhibitors in human histiocytic lymphoma cell line U937. Cell Biochem Funct (2009) 27: 503–515.
24. Jacobson J, Duchen MR and Heales SJ: Intracellular distribution of the fluorescent dye nonyl acridine orange responds to the mitochondrial membrane potential: implications for assays of cardiolipin and mitochondrial mass. J Neurochem (2002) 82: 224–233.
25. Sakharov DV, Elstak ED and Chernyak B: Prolonged lipid oxidation after photodynamic treatment. Study with oxidation-sensitive probe C11-BODIPY581/591. FEBS Lett (2005) 579: 1255–1260.
26. Soh N, Ariyoshi T, Fukaminato T, Nakajima H, Nakano K and Imato T: Swallow-tailed perylene derivative: a new tool for fluorescent imaging of lipid hydroperoxides. Org Biomol Chem (2007) 5: 3762–3768.
27. Liu YL, Ang SO, Weigent DA Prchal JT and Bloomer JR: Regulation of ferrochelatase gene expression by hypoxia. Life Sci (2004) 75: 2035–2043.
28. Furukawa T, Wakabayashi K, Tamura A, Nakagawa H, Morishima

Y, Osawa Y and Ishikawa T: Major SNP (Q141K) variant of human ABC transporter ABCG2 undergoes lysosomal and proteasomal degradations. Pharm Res (2009) 26: 469–479.
29. Gewin L and Galloway DA: E box-dependent activation of telomerase by human papillomavirus type 16 E6 does not require induction of c-myc. J Virol (2001) 75: 7198–7201.
30. Laborda J: 36B4 cDNA used as an estradiol-independent mRNA control is the cDNA for human acidic ribosomal phosphoprotein PO. Nucleic Acids Res (1991) 19: 3998.
31. Evseenko DA, Murthi P, Paxton JW, Reid G, Emerald BS, Mohankumar KM, Lobie PE, Brennecke SP, Kalionis B and Keelan JA: The ABC transporter BCRP/ABCG2 is a placental survival factor, and its expression is reduced in idiopathic human fetal growth restriction. FASEB J (2007) 21: 3592–3605.
32. Juzenas P, Juzeniene A and Moan J: Deferoxamine photosensitizes cancer cells in vitro. Biochem Biophys Res Commun (2005) 332: 388–391.
33. Ding Y, Lin B and Huie CW: Binding studies of porphyrins to human serum albumin using affinity capillary electrophoresis. Electrophoresis (2001) 22: 2210–2216.
34. Solazzo M, Fantappiè O, D'Amico M, Sassoli C, Tani A, Cipriani G, Bogani C, Formigli L and Mazzanti R: Mitochondrial expression and functional activity of breast cancer resistance protein in different multiple drug-resistant cell lines. Cancer Res (2009) 69: 7235–7242.
35. Sharma S, Jajoo A and Dube A: 5-Aminolevulinic acid-induced protoporphyrin-IX accumulation and associated phototoxicity in macrophages and oral cancer cell lines. J Photochem Photobiol B (2007) 88: 156–162.
36. Wyld L, Burn JL, Reed MW and Brown NJ: Factors affecting aminolaevulinic acid-induced generation of protoporphyrin IX. Br J Cancer (1997) 76: 705–712.
37. Schoenfeld N, Mamet R, Nordenberg Y, Shafran M, Babushkin T and Malik Z: Protoporphyrin biosynthesis in melanoma B16 cells stimulated by 5-aminolevulinic acid and chemical inducers: characterization of photodynamic inactivation. Int J Cancer (1994) 56: 106–112.
38. Fukuda H, Batlle AM and Riley PA: Kinetics of porphyrin accumulation in cultured epithelial cells exposed to ALA. Int J Biochem (1993) 25: 1407–1410.
39. Cosserat-Gerardin I, Bezdetnaya L, Notter D, Vigneron C and Guillemin F: Biosynthesis and photodynamic efficacy of protoporphyrin IX (PpIX) generated by 5-aminolevulinic acid (ALA) or its hexylester (hALA) in rat bladder carcinoma cells. J Photochem Photobiol B (2000) 59: 72–79.
40. Selbo PK, Kaalhus O and Sivam G: 5-Aminolevulinic acid-based photochemical internalization of the immunotoxin MOC31-gelonin generates synergistic cytotoxic effects in vitro. Photochem Photobiol (2001) 74: 303–310.
41. Zhou S, Zong Y, Ney PA, Nair G, Stewart CF and Sorrentino BP: Increased expression of the Abcg2 transporter during erythroid maturation plays a role in decreasing cellular protoporphyrin IX levels. Blood (2005) 105: 2571–2576.
42. Desuzinges-Mandon E, Arnaud O, Martinez L, Huché F, Di Pietro A and Falson P: ABCG2 transports and transfers heme to albumin through its large extracellular loop. J Biol Chem (2010) 285: 33123–33133.
43. Chen HM, Liu CM, Yang H, Chou HY, Chiang CP and Kuo MY: 5-aminolevulinic acid induce apoptosis via NF-κB/JNK pathway in human oral cancer Ca9-22 cells. J Oral Pathol Med (2011) 40: 483–489.
44. Furre IE, Møller MT, Shahzidi S Nesland JM and Peng Q: Involvement of both caspase-dependent and -independent pathways in apoptotic induction by hexaminolevulinate-mediated photodynamic therapy in human lymphoma cells. Apoptosis (2006) 11: 2031–2042.
45. Ji HT, Chien LT, Lin YH, Chien HF and Chen CT: 5-ALA mediated photodynamic therapy induces autophagic cell death via AMP-activated protein kinase. Mol Cancer (2010) 9: 91.
46. Gottlieb E, Vander H MG and Thompson CB: Bcl-x(L) prevents the initial decrease in mitochondrial membrane potential and subsequent reactive oxygen species production during tumor necrosis factor alpha-induced apoptosis. Mol Cell Biol (2000) 20: 5680–5689.
47. Karthein R, Dietz R, Nastainczyk W, and Ruf HH: Higher oxidation states of prostaglandin H synthase. EPR study of a transient tyrosyl radical in the enzyme during the peroxidase reaction. Eur J Biochem (1988) 171: 313–320.
48. Akita Y, Kozaki K, Nakagawa A, Saito T, Ito S, Tamada Y, Fujiwara S, Nishikawa N, Uchida K, Yoshikawa K, Noguchi T, Miyaishi O, Shimozato K, Saga S and Matsumoto Y: Cyclooxygenase-2 is a possible target of treatment approach in conjunction with photodynamic therapy for various disorders in skin and oral cavity. Br J Dermatol (2004) 151: 472–480.